Miscibility gap in electrochemically oxygenated $La_2CuO_{4+\delta}$

P. G. Radaelli
Science and Technology Center for Superconductivity, Argonne National Laboratory, Argonne, Illinois 60439

J. D. Jorgensen and R. Kleb
Materials Science Division, Argonne National Laboratory, Argonne, Illinois 60439

B. A. Hunter
Science and Technology Center for Superconductivity, Argonne National Laboratory, Argonne, Illinois 60439

F. C. Chou and D. C. Johnston
Ames Laboratory and Department of Physics and Astronomy, Iowa State University, Ames, Iowa 50011
(Received 5 November 1993)

The miscibility gap of $La_2CuO_{4+\delta}$ was investigated by studying three electrochemically oxygenated samples with different oxygen contents, using variable-temperature neutron powder diffraction. The low-temperature lattice parameters of the two coexisting orthorhombic phases (antiferromagnetic, *Bmab* and superconducting, *Fmmm*) were found to be in good agreement with those determined for high-pressure annealed samples, indicating that the two techniques yield essentially identical samples, at least in this concentration range. A sample with $\delta \approx 0.032$ remained phase separated up to 415 K and, above this temperature, was found to be single-phase tetragonal (*F4/mmm*). The phase separation temperature and the orthorhombic-to-tetragonal phase transition temperature were obtained for all samples, allowing the shape of the miscibility gap to be determined.

I. INTRODUCTION

Despite its relatively low superconducting critical temperature (≤ 45 K), $La_2CuO_{4+\delta}$ is one of the most extensively studied cuprate superconductors. What makes this system so interesting is the fact that the dopant species (in this case, interstitial oxygen atoms) is mobile at temperatures as low as 200 K.[1,2] Therefore the behavior of $La_2CuO_{4+\delta}$ seems to be the ideal test for theories that, in certain doping regimes, predict a phase separation of the charge carriers into domains with different carrier concentrations.[3] In this case, the mobility of the dopant species would allow the domains to develop into two distinct crystallographic phases with different oxygen compositions. Phase separation between an antiferromagnetic and a superconducting phase is indeed observed in $La_2CuO_{4+\delta}$.[4] However, the phase diagram of the isostructural compound $La_2NiO_{4+\delta}$ also contains oxygen miscibility gaps,[5-7] although no superconductivity is observed in this system.

Until very recently, annealing samples at high temperature (~ 500 °C) in a high oxygen partial pressure was the only known method to intercalate oxygen in $La_2CuO_{4+\delta}$ samples. Because of the miscibility gap in the phase diagram, pressures around 25 kbar are required to obtain single-phase superconducting samples.[8,9] Jorgensen *et al.* studied several powder samples of $La_2CuO_{4+\delta}$, prepared at intermediate pressures and temperatures ($PO_2 \leq 3$ kbar, $T \sim 500$ °C),[4] by neutron powder diffraction, and concluded that the superconducting compound resulted from phase separation near room temperature into two phases, both having the well-known K_2NiF_4 or "2:1:4" structure. The oxygen content of the superconducting phase was estimated at $\delta \approx 0.08$, based on the "lever rule" and on the assumption that the antiferromagnetic insulating phase had $\delta = 0$.[10] Both phases were found to have orthorhombic symmetry, but based on the analysis of systematic absences, the structure of the oxygen-rich phase was concluded to have a higher symmetry (*Fmmm*) than the stoichiometric compound (*Bmab*). It was speculated that the higher symmetry resulted from frustration of the *Bmab* tilt pattern, due to the presence of interstitial oxygen atoms. Samples annealed at higher pressures (~ 25 kbar) contained only one 2:1:4 phase,[8,9] but their relatively poor quality (broad diffraction peaks, presence of non-isostructural impurity phases) made them unsuitable for definitive crystallographic studies. In addition, high-pressure synthesis techniques capable of reaching 25 kbar do not easily allow fine-tuning of the oxygen partial pressure.[11] For these reasons, a complete characterization of the miscibility gap in $La_2CuO_{4+\delta}$ was never attempted.

The development of room-temperature chemical[12,13] and electrochemical[14-17] techniques suitable for inserting oxygen into the 2:1:4 oxides has allowed the synthesis of $La_2CuO_{4+\delta}$ $La_{2-x}Sr_xCuO_{4+\delta}$, and $La_2NiO_{4+\delta}$ with very high values of δ. We have recently studied the structure of electrochemically oxygenated $La_2CuO_{4+\delta}$ on two powder samples ($\delta \approx 0.08$, $T_c = 32$ K and $\delta \approx 0.12$, $T_c = 44$ K and on a single crystal ($\delta \approx 0.1$, $T_c = 40$ K) by neutron diffraction.[18] All samples were found to be single phase down to 10–16 K, as evidenced by the sharp Bragg peaks, indicating that these samples had compositions beyond the phase-separated region of the phase diagram. The basic crystallographic structure of all samples had *Fmmm* symmetry, with the excess oxygen located between adjacent LaO layers. However, the presence of sa-

tellite reflections in both powder and single-crystal data evidenced the existence of a large superstructure.

The electrochemical oxidation technique allows fine-tuning of the oxygen content of 2:1:4 oxides. This can be readily accomplished by varying the total amount of anodic current passed through the samples. Therefore, by using this technique, the entire structural phase diagram of $La_2CuO_{4+\delta}$ can be mapped by studying a series of samples with variable composition. A critical point to be addressed is the comparison between $La_2CuO_{4+\delta}$ samples with the same value of δ but prepared with different methods (high-pressure annealing vs electrochemical oxidation). Since electrochemical intercalation of oxygen takes place at room temperature, the configuration of interstitial oxygen atoms and the structural relaxation around them could result in a metastable state, and therefore, electrochemically oxygenated samples could be considerably different from oxygen-annealed samples, where the structure is presumably closer to equilibrium.

In this paper we present structural refinements of neutron-diffraction data at variable temperature on three electrochemically oxygenated powder samples of $La_2CuO_{4+\delta}$ ($\delta \approx 0.018$, 0.032, and 0.044), with compositions within the miscibility gap. The low-temperature compositions of the antiferromagnetic and superconducting phases, estimated using the "lever rule," are 0.012 and 0.055, respectively. The lattice constants of the two phases at low temperature are very close to those of phase-separated samples prepared by high-pressure oxygen annealing, indicating that, at least for this range of oxygen concentrations, the two techniques yield essentially identical samples. The $\delta \approx 0.032$ sample remained phase separated up to 415 K. At higher temperatures, this sample was found to be single-phase tetragonal (*F4/mmm*). From the present data, the miscibility gap of $La_2CuO_{4+\delta}$ was determined to have a pronounced "cusp," possibly related to an additional ordering transition in the *Fmmm* phase.

II. SAMPLE PREPARATION AND CHARACTERIZATION

Three samples of $La_2CuO_{4+\delta}$ with variable oxygen contents were prepared using the electrochemical oxidation technique. The details of the sample preparation are described elsewhere.[17,18] The oxygen contents of the three samples were measured using thermogravimetric analysis (TGA). About 20 mg of powder was heated under 1 atom He gas, and the value of δ was determined from the weight loss between ~ 180 and ~ 380 °C.[17,18] The oxygen contents of the three samples were found to be $\delta = 0.018$, 0.032, and 0.044. The uncertainty of the TGA measurement, which includes both systematic and random errors, was estimated to be ± 0.010.

Field-cooled (FC) and zero-field-cooled (ZFC) dc magnetization measurements in low field (50 Oe) were performed on all samples, using a superconducting quantum interference device (SQUID) magnetometer. As already reported,[1,2,19–24] the value of the onset critical temperature T_c depends on the cooling rate, being 4–5 K higher for slow-cooled samples. As an example, dc susceptibility

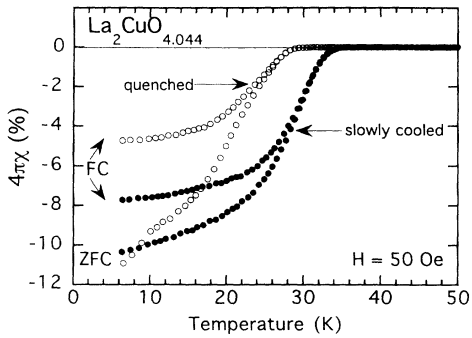

FIG. 1. Field-cooled (FC) and zero-field cooled (ZFC) magnetic susceptibilities χ vs temperature for a $La_2CuO_{4.044}$ powder sample, in a 50-Oe applied magnetic field. No demagnetization corrections were applied. All the data were taken upon warming after the sample was quenched (circles) or slowly cooled (squares) from room temperature to 6 K. The cooling rate for quenching was ~ 100 K/min. The slow-cooling process was done in steps of 5 K, with an average cooling rate of ~ 0.4 K/min.

FC and ZFC curves for the $\delta \approx 0.044$ sample are shown in Fig. 1 both for fast cooling (~ 100 K/min) and for slow cooling (~ 0.4 K/min). The onset T_c's for fast/slow cooling were found to be 32/36, 30/34, and 29/34 K for the $\delta \approx 0.018$, 0.032, and 0.044 samples, respectively.

For comparison, a stoichiometric $La_2CuO_{4+\delta}$ sample was also prepared by annealing in pure N_2 gas at 700 °C, followed by rapid quenching to room temperature. Previous studies have shown[4] that this method produces samples with $\delta = 0.00$, within the experimental errors.

III. NEUTRON DIFFRACTION

Neutron-powder-diffraction data were collected on all powder samples at variable temperature, using the special environment powder diffractometer (SEPD) at Argonne's Intense Pulsed Neutron Source (IPNS).[25] The instrument was equipped with a closed-cycle helium refrigerator (Displex), the head of which was modified to allow heating above room temperature. Typical cooling and heating rates were 2–3 K/min. The instrument temperature calibration was confirmed in a separate experiment using the thermal expansion of NaCl.[26] The maximum attainable temperature in this system is limited by the melting point of cadmium (321 °C), which was used for neutron shielding. For $La_2CuO_{4+\delta}$, TGA experiments have indicated[18] that loss of oxygen starts occurring around 180 °C. Therefore this temperature was never exceeded in our experiments for oxygenated samples. The samples were contained in vanadium tubes sealed under a helium atmosphere, using a lead gasket. For comparison, a sample of stoichiometric $La_2CuO_{4+\delta}$ was run under identical conditions.

The powder-diffraction data were analyzed with the Rietveld technique, using the IPNS code.[27,28] Only data from the high-resolution backscattering detector banks ($2\theta = 148°$) were used in the refinements.

Three phases were observed in the phase diagram: the so-called high-temperature tetragonal (HTT) phase and the two low-temperature orthorhombic phases: *Bmab* and *Fmmm* (No. 69). In order to obtain a consistent set of lattice parameters for the three phases, we used the nonstandard space group *Bmab* instead of the standard *Cmca* (No. 64). Likewise, the nonstandard *F4/mmm* was used for the HTT phase instead of the standard *I4/mmm* (No 139).

Figure 2 shows portions of the raw data and Rietveld refinement profiles for the $\delta \approx 0.018$, 0.032, and 0.044 samples at 200 K. It is clear from inspection of the raw data that all three samples are phase separated into two orthorhombic phases and that the relative amount of the two phases varies with composition. Refinements of the low-temperature data, based on a two-phase model (*Bmab*+*Fmmm*; see below), yield a ratio between the amounts of the two phases of 85(2):15(2)%, 55(1):45(1)%, and 25(1):75(1)% for the $\delta \approx 0.018$, 0.032, and 0.044 samples, respectively. These ratios are essentially temperature independent below 200 K. Using the "lever rule," we can estimate the oxygen content of the two phases δ_{Bmab} and δ_{Fmmm} from the formula

$$\delta_{\text{tot}} = \delta_{Bmab} + (\delta_{Fmmm} - \delta_{Bmab}) f_{Fmmm} ,$$

where δ_{tot} is the total oxygen content of each sample and f_{Fmmm} is the fraction of *Fmmm* phase in that sample. Using a linear regression of the values for the three samples, we determined the oxygen contents of the two phases to be $\delta_{Bmab} = 0.012$ and $\delta_{Fmmm} = 0.055$ at low temperature. The standard deviation on these values estimated from the linear fit alone (± 0.001) is approximately 10 times smaller than the estimated error bars on the measured values of δ, indicating that systematic errors are probably the dominant contribution to the uncertainty in the oxygen contents. For this reason, we chose to report oxygen contents to the third decimal place, and we have omitted the estimated error bars (~ 0.012) based on the propagation of the errors in the TGA measurements.

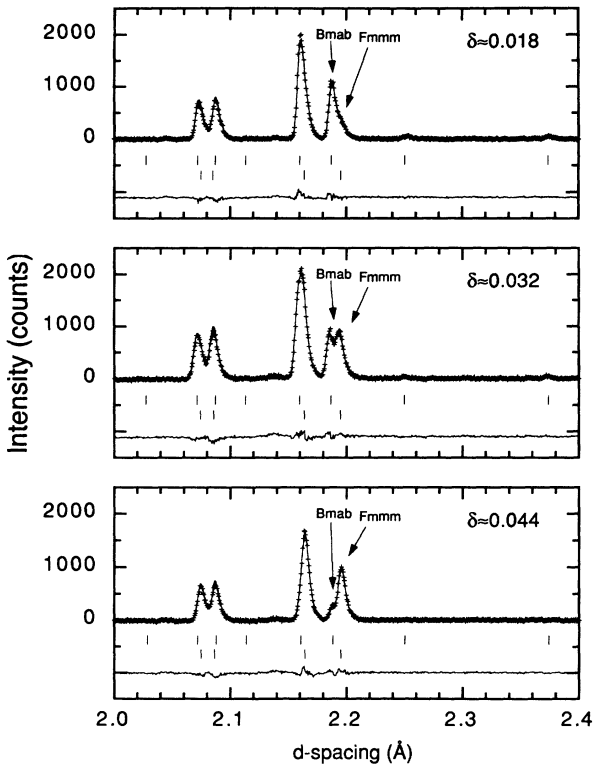

FIG. 2. Sections of the two-phase Rietveld refinement profiles for the $\delta \approx 0.018$ (top), $\delta \approx 0.032$ (middle), and $\delta \approx 0.044$ (bottom) samples at 200 K. The plus (+) signs are the raw time-of-flight neutron-powder-diffraction data. The solid line is the calculated profile. Tick marks below the diffraction profile mark the position of allowed Bragg reflection for the *Bmab* (top) and *Fmmm* (bottom) phases. A difference curve (observe minus calculated) is also plotted. The arrows indicate the positions of the [0,0,6] Bragg reflections for the two phases.

The temperature dependence of the internal parameters is not the subject of this work. However, due to the high degree of correlation, especially near the phase-separation temperature, it is important to use accurate atomic positions in the refinements, even though only lattice parameters and phase fractions are sought. In order to determine atomic positions for samples with two coexisting phases, the following strategy was adopted. A first set of Rietveld refinements was carried out for the $\delta = 0.018$ and 0.044 samples. For the 50-K data, the starting values of the structural parameters were obtained from previous experiments on single-phase samples.[18] Lattice constants and phase fractions were refined for both phases, while the atomic positions were refined only for the majority phase. Once these refinements converged, new refinements were carried out using, for the minority phase, the structural parameters previously refined for the *other* sample. The whole process was repeated, until no change in the structural parameters occurred, within the error bars. For the $\delta \approx 0.032$ sample, only lattice parameters and phase fractions were refined for both phases, while the atomic positions were fixed at the values obtained for the other two samples. A peak width parameter σ_1,[25] which was constrained to be identical for both phases, was also refined for all samples. Once satisfactory structural parameters for a given temperature were obtained, they were used as starting values for the next temperature.

Near the phase-separation temperature, a consistent criterion must be adopted in order to determine whether one or two phases are present. Since the number of parameters is greatly different between single-phase and two-phase models, a comparison of the R values has little meaning, unless a significance test is performed. As an alternative, we preferred to adopt a criterion based on the peak widths. When two-phase samples are analyzed as single phase, the peak width parameter σ_1 converges to a high value to account for the additional broadening. Therefore, for each sample, the intrinsic value of the peak broadening parameter σ_1^0, was first determined from a low-temperature two-phase refinement. At each given temperature, we choose to define a sample as single phase when σ_1, as determined from a single-phase refinement,

was not greater than σ_1^0.

The lattice parameters as a function of temperature, both in the two-phase and single-phase regions, are plotted in Figs. 3, 4, 5, and 6 for the $\delta \approx 0.0$, 0.018, 0.032, and 0.044 samples, respectively. For the $\delta \approx 0.0$, 0.018 compositions, the samples remained orthorhombic throughout all our temperature range, and the position of the orthorhombic-to-tetragonal (OT) phase transitions were estimated by a linear extrapolation. For the $\delta \approx 0.0$ sample, the extrapolated value of the OT temperature (T_{OT}) is ~530 K, which is in good agreement with previous reports.[29–31] T_{OT} decreases with increasing δ, and tetragonal symmetry was attained in our experiment for the $\delta \approx 0.032$ and 0.044 samples. For these phase-separated samples, the values of the low-temperature lattice constants are very similar to those previously reported for phase-separated samples obtained by high-pressure annealing.[4] This confirms that electrochemically oxygenated samples are not qualitatively different from samples obtained by more conventional techniques, at least in this concentration range.

Both the $\delta \approx 0.018$ and 0.044 samples phase separate around room temperature into two orthorhombic phases (*Bmab* + *Fmmm*). Above the phase-separation temperature, these samples are single-phase orthorhombic (*Bmab* for the $\delta \approx 0.018$ sample and *Fmmm* for the $\delta \approx 0.044$ sample). In contrast, the $\delta \approx 0.032$ sample remains two phase up to ~415 K. The *a* and *b* lattice parameters of the *Fmmm* phase refined to identical values within the error bars above ~380 K, suggesting a transition to a tetragonal phase. An individual peak deconvolution analysis also indicated that an orthorhombic (*Bmab*) and a tetragonal phase coexist in the temperature range $380 \leq T \leq 415$ K. Above 415 K the $\delta \approx 0.032$ sample was found to be single-phase tetragonal.

The refined values of the *Bmab* and *Fmmm* phase fractions as a function of temperature for the $\delta \approx 0.032$ and 0.044 samples are shown in Figs. 7 and 8, respectively. For the $\delta \approx 0.032$ sample, the fractions of the two phases remain nearly constant around the low-temperature values up to the phase-separation temperature. It is difficult to judge whether the small fluctuations above 250 K reflect a real change in phase fractions or are due to

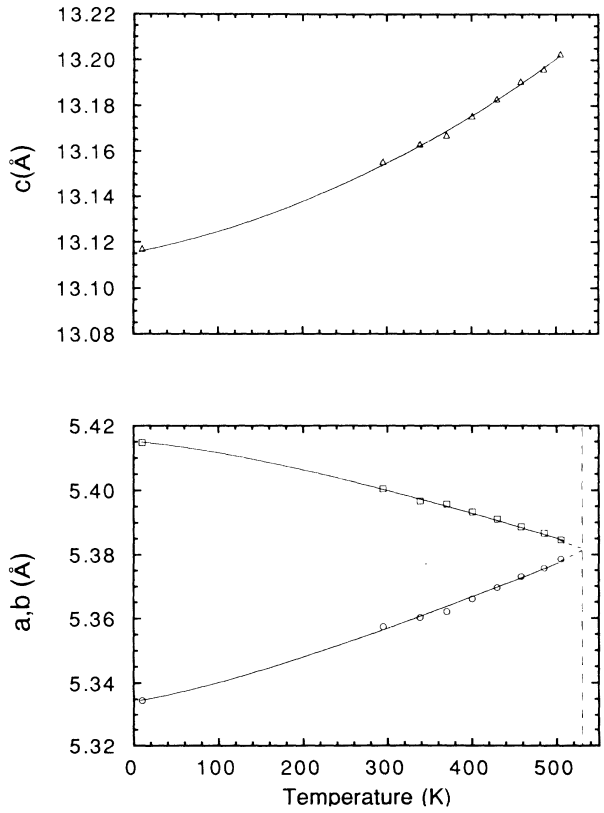

FIG. 3. Lattice parameters *a* (circles), *b* (squares), and *c* (triangles) as a function of temperature for a stoichiometric La_2CuO_4 sample, as determined from Rietveld refinements of neutron-powder-diffraction data. Statistical error bars are smaller than the symbols. The vertical dashed line indicates the extrapolated value of the orthorhombic-to-tetragonal (OT) phase transition temperature. Lines between the points are guides to the eye.

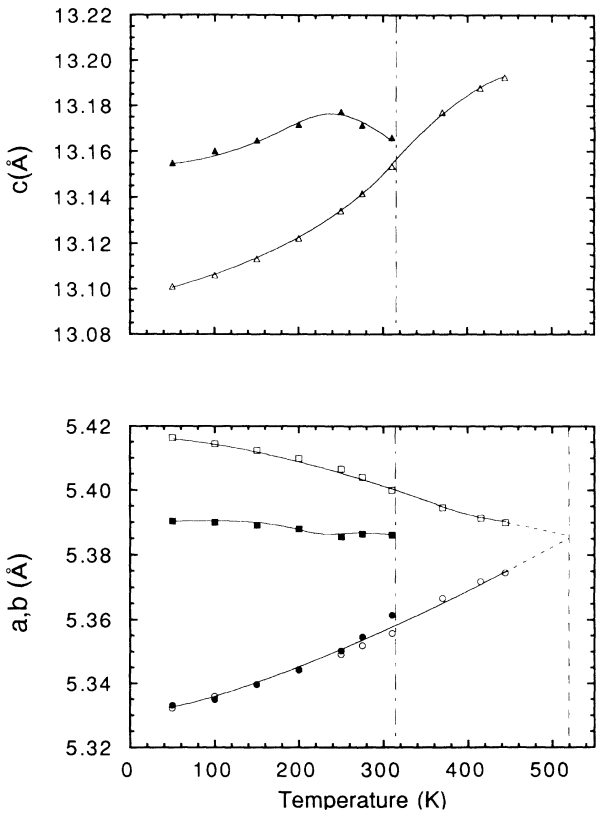

FIG. 4. Lattice parameters as a function of temperture for a $La_2CuO_{4.018}$ sample, as determined from Rietveld refinements of neutron-powder-diffraction data. The symbols indicate *a* (*Bmab*) (open circles), *b* (*Bmab*) (open squares), *c* (*Bmab*) (open triangles), *a* (*Fmmm*) (solid circles), *b* (*Fmmm*) (solid squares), and *c* (*Fmmm*) (solid triangles). Statistical error bars are smaller than the symbols. The vertical dot-dashed line indicates the estimated phase-separation temperature, above which the sample is single-phase *Bmab*. The vertical dashed line indicates the extrapolated value of the orthorhombic-to-tetragonal (OT) phase transition temperture. Lines between the points are guides to the eye.

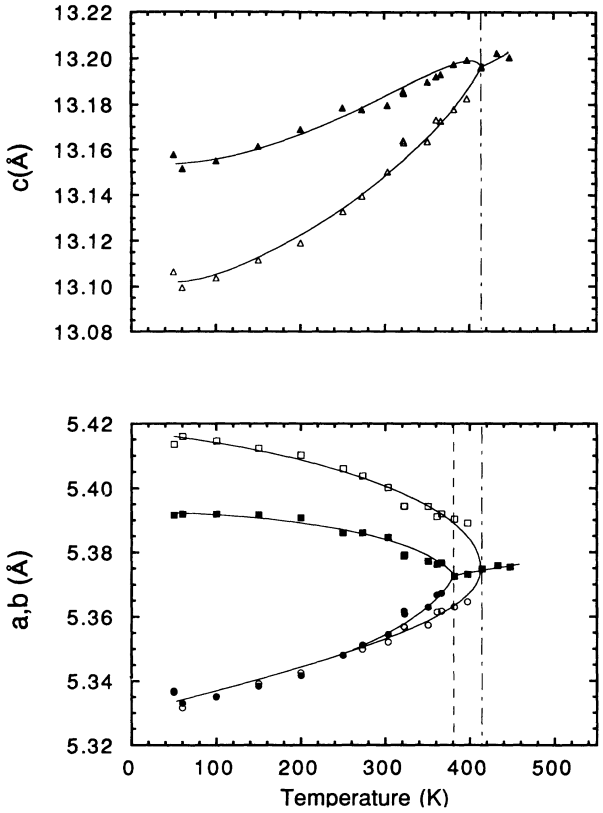

FIG. 5. Lattice parameters as a function of temperature for a $La_2CuO_{4.032}$ sample, as determined from Rietveld refinements of nuetron-powder-diffraction data. The symbols are the same as in Fig. 4. The vertical dot-dashed line indicates the estimated phase-separation temperature, above which the sample is single-phase tetragonal (*F4/mmm*). The vertical dashed line indicates the value of the orthorhombic-to-tetragonal (OT) phase transition temperature for the *Fmmm* phase. Lines between the points are guides to the eye.

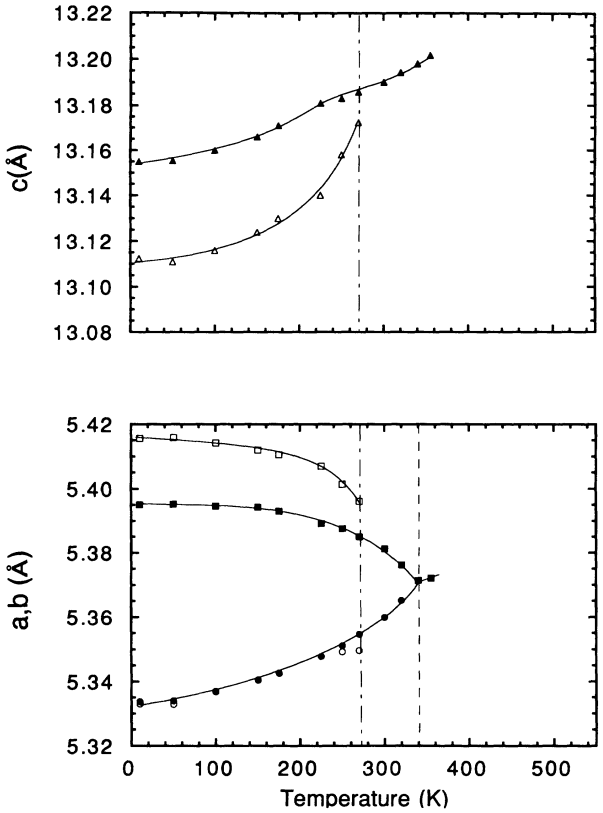

FIG. 6. Lattice parameters as a function of temperature for a $La_2CuO_{4.044}$ sample, as determined from Rietveld refinements of nuetron-powder-diffraction data. The symbols are the same as in Figs. 4 and 5. The vertical dot-dashed line indicates the estimated phase-separation temperature, above which the sample is single-phase orthorhombic (*Fmmm*). The vertical dashed line indicates the value of the orthorhombic-to-tetragonal (OT) phase transition temperature. Lines between the points are guides to the eye.

the increased correlations between the two quasi-isostructural phases. Since the composition of this sample is close to the middle of the phase-separation region, the observed behavior is consistent with a nearly symmetric miscibility gap. For the other two compositions, we expect the fraction of the minority phase to decrease as a function of temperature and to go to zero at the phase-separation temperature, while the lattice parameters of the two phases remain different. The $\delta \approx 0.044$ sample indeed shows the expected behavior (Fig. 8). It is interesting to note that the phase fractions do not change below ~ 200 K, indicating that the miscibility gap has vertical sides at these temperatures. This effect is probably due to the loss of mobility of the interstitial oxygen atoms.

In the attempt to address the question of the cooling-rate dependence of T_c, the $\delta \approx 0.044$ sample was also studied at low temperature (10 K) after slow cooling (0.3 K/min) in the 270–150 K temperature range, where the cooling rate is known to affect T_c.[2,23] However, no

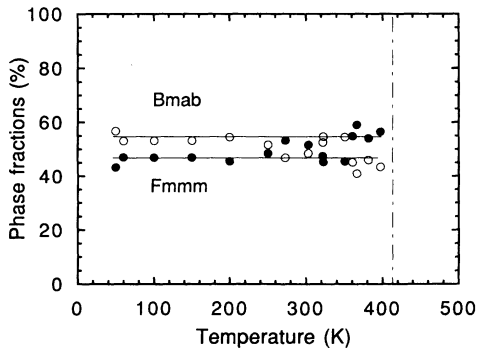

FIG. 7. Phase fraction of the *Bmab* (open circles) and *Fmmm* (solid circles) phases as a function of temperature for the $La_2CuO_{4.032}$ sample, as determined from neutron-powder-diffraction data. The vertical dot-dashed line indicates the estimated phase-separation temperature. Lines between the points are guides to the eye.

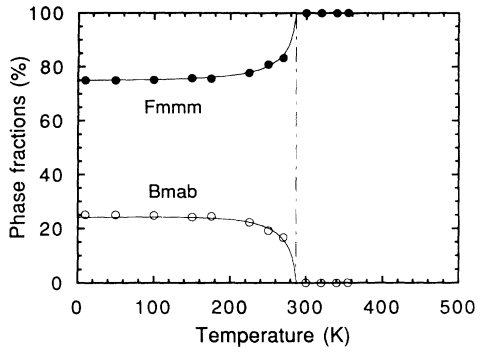

FIG. 8. Phase fraction of the *Bmab* (open circles) and *Fmmm* (solid circles) phases as a function of temperature for the $La_2CuO_{4.044}$ sample, as determined from neutron-powder-diffraction data. The vertical dot-dashed line indicates the estimted phase-separation temperature. Lines between the points are guides to the eye.

significant differences in the structural parameters, as well as in the fractions of the two phases, were observed in comparison to a fast-cooled sample (~ 3 K/min). This observation may indicate that the reduced T_c for fast-cooling samples is not due to incomplete phase separation. Another possibility is that our "fast" cooling rate is not fast enough to reproduce the effect of true quenching.

For the $\delta \approx 0.018$ sample, we were unable to detect any significant change in phase fractions at temperatures approaching phase separation. Rather, at the phase separation temperature, the refined lattice parameters of the minority phase appear to merge with those of the majority phase. This behavior is clearly unphysical and is likely due to a high degree of correlation between parameters in the least-squares procedure. In fact, due to the relative position of the Bragg peaks of the various phases, it is more difficult to accurately determine phase fractions when the minority phase has a smaller orthorhombic strain than the majority phase.

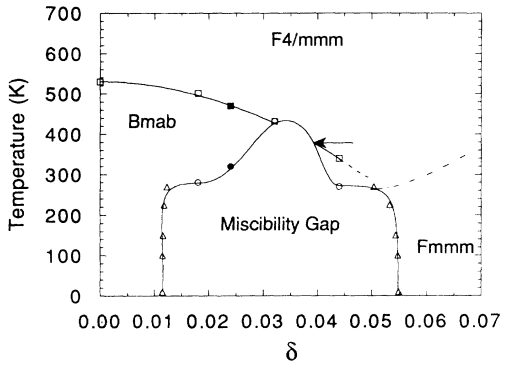

FIG. 9. Phase diagram of $La_2CuO_{4+\delta}$ in the region of the miscibility gap, as determined from the present study. Open circles and squares indicate the phase separation tempertures and the OT phase transition temperatures, respectively, as determined from neutron-powder-diffraction data. The arrow indicates the OT phase transition temperature of the *Fmmm* phase for the phase-separated $\delta \approx 0.032$ sample. Triangles indicate the sides of the miscibility gap at various temperatures, as determined by applying the "lever rule" to the $\delta \approx 0.018$ and 0.044 samples. The solid circle and square indicate the phase separation temperature and the OT phase transition temperature, respectively, for the high-pressure annealed sample studied in Ref. 4. Since the determination of the oxygen content for this sample was performed using a different method (total weight loss after nitrogen reduction), the abscissa for this sample was established based on the *Bmab*:*Fmmm* phase fractions from neutron powder diffraction. Lines between the points are guides for the eye. The dot-dashed line indicates the position of a possible additional phase line, discussed in the text.

Figure 9 shows the phase diagram of $La_2CuO_{4+\delta}$ in the region of miscibility gap, as determined using the present data. All points below 250 K (triangles) were established using "the lever rule" for the $\delta \approx 0.018$ and 0.044 samples. The phase-separation temperature and orthorhombic-to-tetragonal (OT) phase transition temperature for the high-pressure annealed sample of Ref. 4 were also included in the plot (solid circle and square, respectively). Since the oxygen content of this sample was not determined in a consistent manner with the other samples, its horizontal position on the phase diagram was defined based on the ratio between the fraction of the two phases, as determined from neutron diffraction.

IV. DISCUSSION

The most striking feature of the phase diagram in Fig. 9 is the presence of a pronounced cusp in the miscibility gap. This feature can be observed only by studying samples near the 50:50% composition and is inaccessible for samples closer to the edges of the miscibility gap. Therefore our results are not in contrast with the nuclear magnetic resonance (NMR) and nuclear quadrupole resonance (NQR) data obtained by Hammel *et al.*[2] In fact, the samples studied by Hammel *et al.* were phase separated at low temperature in the ratio $\sim 75{:}25\%$, and were single phase above ~ 270 K. By studying such samples alone, no conclusion can be made about the shape of the miscibility gap above their phase-separation temperature.

Miscibility gaps with cusps are common in the phase diagrams of binary systems, both in the liquid (e.g., In-V and in the solid phase (e.g., Zr-Ta),[32] and are generally associated with the presence of a monotectic point in the phase diagram. In the In-V system, for example, the homogeneous liquid has a miscibility gap with apex at 2560 °C. The indium-rich compositions (L_1) remain liquid down to low temperatures, while the vanadium-rich liquid (L_2) solidifies around 1900 °C. At the monotectic temperature (1877 °C), where L_1, L_2, and the solid are in equilibrium, the slope of the phase lines changes suddenly, and, on the V-rich side, a discontinuity is present, due to the different solubility of indium in the liquid and in the solid phases. Similar behavior is displayed by the Zr-Ta system. However, in this case, the homogeneous phase is a solid solution (β—Zr, Ta) instead of a liquid.

The unusual shape of the miscibility gap of $La_2CuO_{4+\delta}$ as determined by the present data, suggests that a solid-state monotectic transition may occur. It is tempting to correlate this hypothesis with the observation of addi-

tional ordering in the *Fmmm* phase by electron diffraction[13,15] and single-crystal neutron diffraction.[18] In fact, the monotectic transition could be due to ordering of the interstitial oxygen atoms and/or of the associated atomic displacement field in the *Fmmm* phase. An additional suggestion that this behavior might occur is provided by the observation that the OT phase transition temperature continues to decrease in the *Fmmm* phase for $\delta \leq 0.05$. However, previous studies[15,18] have shown that samples with higher oxygen contents are still orthorhombic at room temperature. Furthermore, the orthorhombic strain at room temperature for a $\delta \approx 0.12$ sample was found to be larger than for the stoichiometric compound ($\delta = 0$),[18] suggesting that, for higher values of the oxygen concentration, the OT phase transition temperature may increase with increasing δ. These observations imply the presence of a minimum in the OT phase transition line. The increased stability of the orthorhombic phase over the tetragonal phase for high values of δ would be consistent with the presence of an ordering transition.

Direct evidence of additional phase lines in the phase diagram is not provided by the present data and must be sought by studying samples past the right edge of the miscibility gap. However, this work indicates that the phase diagram of $La_2CuO_{4+\delta}$ is more complex than previously thought and suggests that additional ordering phenomena must be investigated as an important element in determining the structural and superconducting properties of this compound.

ACKNOWLEDGMENTS

This work was supported by the National Science Foundation Office of Science and Technology Centers under Contract No. DMR 91-20000 (P.G.R., B.A.H) and by the U.S. Department of Energy, Basic Energy Sciences-Materials Sciences, under Contract No. W-31-109-ENG-38 (J.D.J., R.K.). Ames Laboratory is operated for the U.S. Department of Energy by Iowa State University under Contract No. W-7405-ENG-82. The work at Ames (F.C.C., D.C.J.) was supported by the Director for Energy Research, Office of Basic Energy Sciences. We wish to thank David Hinks for his contribution of ideas and discussions.

[1]R. K. Kremer, E. Sigmund, V. Hizhnyakov, F. Hentsch, A. Simon, K. A. Muller, and M. Mehring, Z. Phys. B **86**, 319 (1992).

[2]P. C. Hammel, E. T. Ahrens, A. P. Reyes, J. D. Thompson, D. E. MacLaughlin, Z. Fisk, P. C. Canfield, and J. E. Schirber, in *Phase Separation in Cuprate Superconductors,* Erice, Italy, 1992, edited by K. A. Muller and G. Benedek (World Scientific, Singapore, 1993), p. 139.

[3]V. J. Emery and S. A. Kivelson, Physica C **209**, 597 (1993).

[4]J. D. Jorgensen, B. Dabrowski, S. Pei, D. G. Hinsk, L. Soderholm, B. Morosin, J. E. Schirber, E. L. Venturini, and D. S. Ginley, Phys. Rev. B **38**, 11 337 (1988).

[5]J. D. Jorgensen, B. Dabrowski, S. Pei, D. R. Richards, and D. G. Hinks, Phys. Rev. B **40**, 2187 (1989).

[6]D. J. Buttrey, P. Ganguly, J. M. Honig, C. N. R. Rao, R. R. Schartman, and G. N. Subbanna, J. Solid State Chem. **74**, 233 (1988).

[7]D. E. Rice and D. J. Buttrey, J. Solid State Chem. **105**, 197 (1993).

[8]J. Zhou, S. Sinha, and J. B. Goodenough, Phys. Rev. B **39**, 12 331 (1989).

[9]J. D. Jorgensen, B. Dabrowski, D. G. Hins, S. Pei, H. B. Vanfleet, and D. L. Decker (unpublished).

[10]B. Dabrowski, J. D. Jorgensen, D. G. Hinks, S. Pei, D. R. Richards, H. B. Vanfleet, and D. L. Decker, Physica C **162-164**, 99 (1989).

[11]J. E. Schirber, W. R. Bayless, F. C. Chou, D. C. Johnston, P. C. Canfield, and Z. Fisk, Phys. Rev. B **48**, 6506 (1993).

[12]P. Rudolf and R. Schöllhorn, J. Chem. Soc., Chem. Commun. **1992**, 1158 (1992).

[13]E. Takayama-Muromachi, T. Sasaki, and Y. Matsui, Physica C **207**, 97 (1993).

[14]A. Wattiaux, J. C. Park, J.-C. Grenier, and M. Pouchard, C. R. Acad. Sci. Ser. 2 **310**, 1047 (1990).

[15]J.-C. Grenier, A. Wattiaux, and M. Pouchard, in *Phase Separation in Cuprate Superconductors,* Erice, Italy, 1992, edited by K. A. Muller and G. Benedek (World Scientific, Singapore, 1993), p. 187.

[16]J.-C Grenier, N. Lagueyte, A. Wattiaux, J.-P. Doumerc, P. Dordor, J. Etourneau, M. Pouchard, J. B. Goodenough, and J. S. Zhou, Physica C **202**, 209 (1992).

[17]F. C. Chou, J. H. Cho, and D. C. Johnston, Physica C **197**, 303 (1992).

[18]P. G. Radaelli, J. D. Jorgensen, A. J. Schultz, B. A. Hunter, J. L. Wagner, F. C. Chou, and D. C. Johnston, Phys. Rev. B **48**, 499 (1993).

[19]R. Yoshizaki, H. Sawada, T. Iwazumi, and H. Ikeda, Solid State Commun. **65**, 1539 (1988).

[20]R. Yoshizaki, H. Sawada, T. Iwazumi, and H. Ikeda, Physica C **153-155**, 1495 (1988).

[21]R. Yoshizaki, H. Sawada, T. Iwazumi, and H. Ikeda, Synth. Met. **29**, F735 (1989).

[22]A. Sulpice, P. Lejay, R. Tournier, B. Chevalier, G. Demazeau, and J. Etourneau, Physica B **165&166**, 1157 (1990).

[23]E. T. Ahrens, A. P. Reyes, P. C. Hammel, J. D. Thompson, P. C. Canfield, Z. Fisk, and J. E. Schirber, Physica C **212**, 317 (1993).

[24]M. Mehring, M. Baehr, P. Gergen, J. Gross, C. Kessler, and N. Winzek, in *Phase Separation in Cuprate Superconductors,* Erice, Italy, 1992, edited by K. A. Muller and G. Benedek (World Scientific, Singapore, 1993), p. 67.

[25]J. D. Jorgensen, J. Faber, Jr., J. M. Carpenter, R. K. Crawford, J. R. Haumann, R. L. Hitterman, R. Kleb, G. E. Ostrowski, F. J. Rotella, and T. G. Worlton, J. Appl. Crystallogr. **22**, 321 (1989).

[26]F. D. Enck and J. G. Dommel, J. Appl. Phys. **36**, 839 (1965).

[27]R. B. von Dreele, J. D. Jorgensen, and C. J. Windsor, J. Appl. Crystallogr. **15**, 581 (1982).

[28]F. J. Rotella, *User manual for Rietveld analysis of time-of-flight neutron powder diffraction data at IPNS* (Intense Pulsed Neutron Source, Argonne National Laboratory, Argonne, IL, 1988).

[29]J. M. Longo and P. M. Raccah, J. Solid State Chem. **6**, 526 (1973).

[30]M. Kato, Y. Maeno, and T. Fujita, Physica C **152**, 116 (1988).

[31]D. Vaknin, S. K. Sinha, D. E. Moncton, D. C. Johnston, J. M. Newsam, C. R. Safinya, and H. E. King, Jr., Phys. Rev. Lett. **58**, 2802 (1987).

[32]T. B. Massalski, *Binary Alloy Phase Diagrams* (ASM International, City, 1990).